Can Resistive Kink Instabilities Drive Simple Loop Flares ?

M. Velli[1], G. Einaudi[2], and A. W. Hood[1]

1 Department of Mathematics, The University
St.Andrews, KY169SS, Fife, Scotland

2 Istituto di Astronomia, Universita' di Firenze, Italy

Summary.

A detailed analysis of the kink instability in finite length (inertially line-tied), cylindrically symmetric coronal loops is presented. The correct line-tying boundary conditions within the framework of ideal and resistive magnetohydrodynamics are discussed, and the growth rates of unstable modes and corresponding eigenfunctions are calculated. Resistive kink modes are found to be unstable in configurations where the axial magnetic field undergoes an inversion, resistive effects being confined to a small region around the loop vertex.

1. Equilibrium and Linearized Equations.

We model coronal loops as axially symmetric, finite length, plasma columns, neglecting the toroidal curvature (which introduces stabilising effects that are second order in the inverse of the loop aspect ratio). Introducing cylindrical coordinates and unit vectors $\mathbf{e}_r$, $\mathbf{e}_\theta$, $\mathbf{e}_z$, the magnetic field may be written as

$$\mathbf{B} = B_\theta(r)\mathbf{e}_\theta + B_z(r)\mathbf{e}_z, \tag{1}$$

and satisfies the static MHD equilibrium condition

$$\frac{\partial}{\partial r}\left(p + \frac{B^2}{8\pi}\right) = -\frac{B_\theta^2}{4\pi r}. \tag{2}$$

A fairly realistic family of equilibrium models is that proposed by Chiuderi et al. (1980), in which a force-free system of currents is continuously matched to an external potential field. The radial structure of the current density $\mathbf{j}$ may be described by

$$\mathbf{j} = \alpha(r)\frac{c\mathbf{B}}{4\pi} \tag{3}$$

where $\alpha(r)$ has the form

$$\alpha(r) = \begin{cases} \alpha_0 & \text{if } r \leq r_0; \\ \frac{\alpha_0}{2}\left(1 + \cos\frac{\pi}{\delta}(r - r_0)\right) & \text{if } r_0 < r \leq r_0 + \delta; \\ 0 & \text{if } r_0 + \delta < r; \end{cases} \tag{4}$$

so that the transition from a force-free to potential configuration is continuous, and no surface currents are present at the boundaries. The photosphere is located at $z = -L$ and $z = L$, a natural measure of the loop length being $l = 2\alpha_0 L$. Two limiting example cases that we will discuss in detail are shown in figure 1. The normalized radius of the current channel is $\alpha_0(r_0 + \delta) = a = 5$; for equilibrium (a) $\alpha_0 r_0 = 0.1$, $\alpha_0\delta = 4.9$, for equilibrium (b) $\alpha_0 r_0 = 2.0$, $\alpha_0\delta = 3.0$. In case (a), there is no inversion in the axial component of the magnetic field, which becomes a very small constant outside the current channel. Linearizing about the static equilibrium, and introducing unit vectors $\mathbf{e}_{||} = \mathbf{B}/B$ and $\mathbf{e}_\perp = (B_z\mathbf{e}_\theta - B_\theta\mathbf{e}_z)/B$ and small perturbations of the form $\bar{\xi}(\mathbf{r}, t) = \bar{\xi}(\mathbf{r})\exp(\gamma t)$, the linearized MHD equations become, in terms of the components $\bar{\xi} = \bar{\xi}\cdot\mathbf{e}_r$, $\bar{\xi}_\perp = \bar{\xi}\cdot\mathbf{e}_\perp$, $\bar{\xi}_{||} = \bar{\xi}\cdot\mathbf{e}_{||}$, $\bar{B}_r$, $\bar{B}_\theta$, $\bar{B}_z$,

$$4\pi\rho\gamma^2\bar{\xi} = \frac{\partial}{\partial r}\left(4\pi\frac{\partial p}{\partial r}\bar{\xi} + 4\pi\gamma_s p\nabla\cdot\bar{\xi} - B_\theta\bar{B}_\theta - B_z\bar{B}_z\right) + \mathbf{B}\cdot\nabla\bar{B}_r - \frac{2B_\theta\bar{B}_\theta}{r}, \tag{5}$$

https://doi.org/10.1017/S0252921100154405 Published online by Cambridge University Press

$$4\pi\rho\gamma^2\tilde{\xi}_\perp = \mathbf{e}_\perp\cdot\nabla(4\pi\frac{\partial p}{\partial r}\tilde{\xi} + 4\pi\gamma_s p\nabla\cdot\tilde{\xi}) + (\mathbf{e}_\perp\cdot\frac{\partial \mathbf{B}}{\partial r} + \frac{B_z B_\theta}{Br})\tilde{B}_r + B\frac{\partial \tilde{B}_\theta}{\partial z} - B\frac{\partial \tilde{B}_z}{\partial \theta}, \quad (6)$$

$$4\pi\rho\gamma^2\tilde{\xi}_\parallel = \mathbf{e}_\parallel\cdot\nabla(4\pi\frac{\partial p}{\partial r}\tilde{\xi} + 4\pi\gamma_s p\nabla\cdot\tilde{\xi}) + \left(\mathbf{e}_\parallel\cdot\frac{\partial \mathbf{B}}{\partial r} + \frac{B_\theta^2}{rB}\right)\tilde{B}_r, \quad (7)$$

$$\tilde{B}_r = \mathbf{B}\cdot\nabla\tilde{\xi} + \frac{\eta c^2}{4\pi\gamma}\left(\nabla^2\tilde{B}_r - \frac{2}{r^2}\frac{\partial \tilde{B}_\theta}{\partial\theta} - \frac{\tilde{B}_r}{r^2}\right), \quad (8)$$

$$\tilde{B}_\theta = \frac{\partial(B\tilde{\xi}_\perp)}{\partial z} - \frac{\partial(B_\theta\tilde{\xi})}{\partial r} + \frac{\eta c^2}{4\pi\gamma}\left(\nabla^2\tilde{B}_\theta + \frac{2}{r^2}\frac{\partial}{\partial\theta}\tilde{B}_r - \frac{\tilde{B}_\theta}{r^2}\right), \quad (9)$$

$$\tilde{B}_z = -\frac{\partial(B\tilde{\xi}_\perp)}{\partial\theta} - \frac{1}{r}\frac{\partial}{\partial r}(B_z r\tilde{\xi}) + \frac{\eta c^2}{4\pi\gamma}\nabla^2\tilde{B}_z, \quad (10)$$

where γ_s is the ratio of the specific heats. In the following, only incompressible modes will be considered. In this case $4\pi\gamma_s p\nabla\cdot\tilde{\xi} \equiv \tilde{\zeta}$ is determined by the additional condition $\nabla\cdot\tilde{\xi} = 0$.

2. Boundary Conditions.

In previous work on the line-tying effect, to sets of boundary conditions have most commonly been used:the flow-through boundary conditions

$$\tilde{\xi}(L) = \tilde{\xi}(-L) = 0,$$

$$\tilde{\xi}_\perp(L) = \tilde{\xi}_\perp(-L) = 0,$$

$$\tilde{\xi}_\parallel(L) = \tilde{\xi}_\parallel(-L),\ \frac{\partial\tilde{\xi}_z}{\partial z}(L) = \frac{\partial\tilde{\xi}_z}{\partial z}(-L), \quad (11)$$

which are compatible with considering incompressible perturbations, and the rigid wall boundary conditions, according to which the parallel component of the perturbed displacement must vanish as well. Although the flow-through boundary conditions have been the subject of some criticism (Low, 1985, Cargill et al., 1986), because they require a strong correlation of what should be arbitrary perturbations across the large distances separating the pairs of footpoints, they give the same results for stability in the case of force-free fields, and result in a noticeable mathematical simplification, so we will use them in the following.

The above boundary conditions are strictly valid only within the framework of ideal MHD, arising from the condition that the jump of the perturbed electric field across the boundary must vanish (which in general, gives rise to a surface current flowing along the boundary). When resistivity is taken into account, the jump in the perturbed magnetic field must vanish as well. However the ideal boundary conditions may still be applied if the distance the surface current diffuses over the time-scale of the instability is much smaller than the loop length scale, a condition which is always satisfied provided the resistive instability grows faster than ordinary diffusion. Hence, we may use (11) for studying both the ideal and resistive situations.

3. Eigenvalue Equations

To obtain an eigenvalue equation from (5)-(10), we expand $\tilde{\xi}$,$\tilde{\xi}_\perp$ and $\tilde{\xi}_\parallel$ in a general Fourier series:

$$\tilde{\xi} = \mathrm{Re}\sum_{n=-\infty}^{\infty}\sum_{m=-\infty}^{\infty}\xi_{nm}(r)\exp[i(m\theta + n\pi(z/L+1))], \quad (12)$$

$$\tilde{\xi}_\perp = \mathrm{Re}\sum_{n=-\infty}^{\infty}\sum_{m=-\infty}^{\infty}\zeta_{nm}(r)\exp[i(m\theta + n\pi(z/L+1)) + i\pi/2] \quad (13)$$

$$\tilde{\xi}_\parallel = \mathrm{Re}\sum_{n=-\infty}^{\infty}\sum_{m=-\infty}^{\infty}\eta_{nm}(r)\exp[i(m\theta + n\pi(z/L+1) + i\pi/2] \quad (14)$$

https://doi.org/10.1017/S0252921100154405 Published online by Cambridge University Press

where n, m are integers. Boundary conditions (11) imply that the Fourier coefficients have to satisfy the constraints

$$\sum_{n=-\infty}^{\infty} \xi_{mn}(r) = 0, \qquad \sum_{n=-\infty}^{\infty} \zeta_{mn}(r) = 0, \tag{15}$$

for all m. Since the boundary constraints (15) are θ-invariant, and therefore do not cause coupling of the harmonics in the angular coordinate, we may restrict consideration to the $m = 1$ kink mode. We then multiply the equations of motion by the phase factor $exp[-i(\theta + n\pi(z/l + 1)]$ and integrate in θ and z. Although the displacement is a periodic function in the axial direction, the line-tying boundary conditions exclude peridicity of its derivatives, so that on integration by parts unknown surface terms arise through which (15) may be applied (details may be found in Velli, Einaudi and Hood, 1988). An infinite set of coupled differential equations in the components ξ_n (along the radial direction) is obtained, which when truncated to N harmonics takes the form (for simplicity we write the ideal MHD equations only, the resistive equations may be found in the above paper; a prime denotes differentiation with respect to r):

$$\left(\left(\frac{f_n^2 + 4\pi\rho\gamma^2}{F_n^2 r}\right)(r\xi_n)'\right)' - (f_n^2 + 4\pi\rho\gamma^2)\xi_n - \left(\frac{B_\theta^2}{r^2} + \frac{2B_\theta}{r}\frac{g_n k_n}{F_n^2}\right)' r\xi_n +$$
$$+ \frac{4B_\theta^2 k_n^2}{r^2 F_n^2 (1 + \frac{4\pi\rho\gamma^2}{f_n^2})}\xi_n + B_z^2\lambda_r - \left(\frac{B g_n}{F_n^2}\lambda_\perp\right)' \quad \frac{2BB_\theta k_n}{r F_n^2 (1 + \frac{4\pi\rho\gamma^2}{f_n^2})}\lambda_\perp = 0, \tag{16}$$

for each n,

$$\lambda_\perp = -\frac{\sum_n^N \left(\frac{g_n}{BrF_n^2}(r\xi_n)' + \frac{2B_\theta k_n}{BrF_n^2(1+\frac{4\pi\rho\gamma^2}{f_n^2})}\xi_n\right)}{\sum_n^N \frac{1}{F_n^2(1+\frac{4\pi\rho\gamma^2}{f_n^2})}}, \tag{17}$$

f_n, g_n are defined from the usual cylindrical pinch analysis ($k_n = n\pi/L$) as

$$f_n = \frac{m}{r}B_\theta + k_n B_z, \quad g_n = \frac{m}{r}B_z - k_n B_\theta. \tag{18}$$

and $F_n^2 = \frac{m^2}{r^2} + k_n^2$ is the square of the total wave-vector. To solve, we eliminate $\xi_N = -\sum_n^{N-1}\xi_n$ and λ_r by subtracting the Nth equation from the remaining N-1. We then select a central wavenumber k_0, corresponding to the fastest growing mode in the infinite pinch, and add sidebands until the solution has sufficiently converged. In practice, 5 modes are sufficient (convergence with increasing N is guaranteed by the properties of the kink mode in the infinite pinch,i.e., that wavenumbers not in a range $0 < |k| < k_c$ are stable).

4. Results and Conclusion

In Figure 2 we show the growth rate of ideal kink modes as a function of inverse loop length for equilibria (a) and (b) described above. The growth rates (which are normalized to the typical Alfvén time $\tau_a = 4\pi\rho/(\alpha_0^2 B_0^2)$), depends very sensitively on the length of the loop, and once the critical lengthis exceeded grows rapidly to $\gamma\tau_a \simeq 10^{-2}$. In Figure 3 ((a) and (b)) the corresponding radial components of the marginal eigenfunctions are plotted as a function of r and z. Although the coupled equations are no longer singular, we find that in case (b), the perturbed magnetic field vanishes along a ring of constant radius r_c at the loop vertex (z=0). In this region resistive effects are important, and we find that, at marginal stability, a resistive kink mode with a scaling $\gamma\tau_a \sim (\tau_a/\tau_r)^\alpha$ where $\alpha \simeq 1/3$ is excited. Equilibria of type (b) are also unstable to m=0 tearing modes, and do not appear to be a realistic model for quasi-static coronal loops. However our results indicate that the interaction of loops could play an important role in the initiation of flares, by providing a region where the field component connecting to the photosphere undergoes an inversion. Results from a more detailed analysis will be presented elsewhere.

References

Cargill,P. J. , Hood,A. W. and Migliuolo,S. : 1986, *Astrophys. J.* 309, 402.

https://doi.org/10.1017/S0252921100154405 Published online by Cambridge University Press

Chiuderi,C. , Einaudi,G. , MA,S.S. and Van Hoven,G. : 1980, *J. Plasma Phys.* **24**,

Low,B. C. : 1985, *Solar Phys.* **100**, 309.

Velli,M. ,Einaudi,G. and Hood,A. W. : 1988, *Astrophys. J.* , , submitted

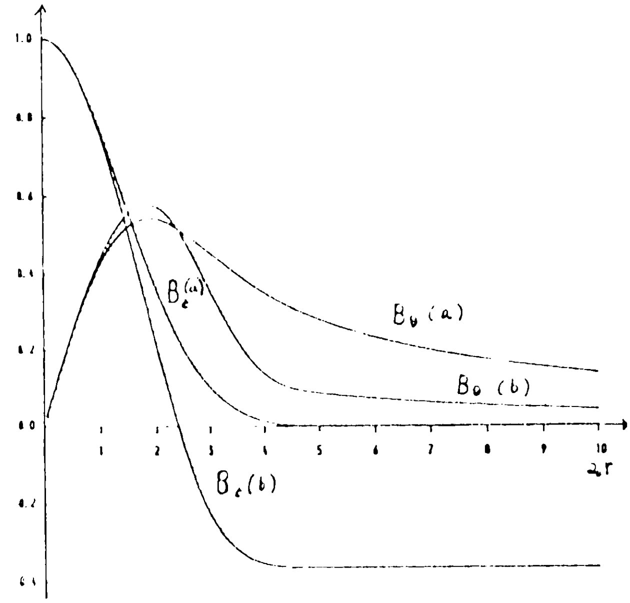

Figure 1. Equilibrium profiles examined for stability: (a) $a_0 r_0 = 0.1$ $a_0 \delta = 4.9$
(b) $a_0 r_0 = 2.0$ $a_0 \delta = 3.0$

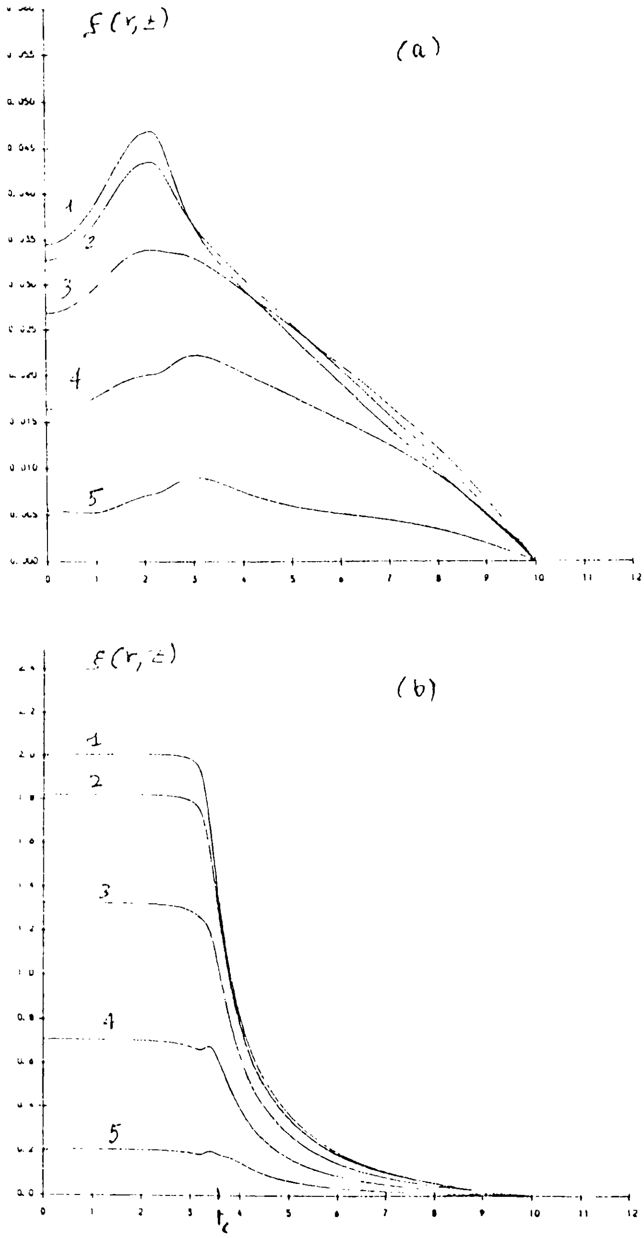

Figure 3. Radial profiles of the perturbed displacement for various values of z. (1) z=0.0 (2)z=0.2L (3)z=0.4L (4)z=0.6L (5)z=0.8L

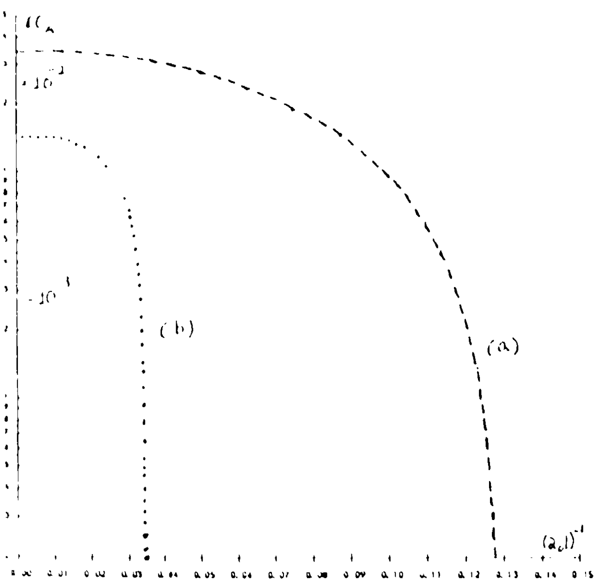

Figure 2. Growth rates of ideal kink modes as a function of the inverse loop length. Curves (a) and (b) correspond to equilibrium (a) and (b) respectively.